Chaos, Solitons and Fractals 190 (2025) 115732

Contents lists available at ScienceDirect

Chaos, Solitons and Fractals

journal homepage: www.elsevier.com/locate/chaos

A thermodynamic model of the REM–NREM sleep cycle

Haeun Sun [a], Yurii Ishbulatov [b,c], Anatoly Karavaev [b,c], Denis Zakharov [d], Alexey Zaikin [d,e,*]

[a] Queen Square Institute of Neurology, University College London, Queen Square, London, WC1N 1PA, United Kingdom
[b] Saratov State University, Astrakhanskaya 83, Saratov, 410012, Russia
[c] Saratov Branch of the Institute of Radio Engineering and Electronics of Russian Academy of Sciences, Zelyonaya 38, Saratov, 410019, Russia
[d] Institute for Cognitive Neuroscience, University Higher School of Economics, 20 Myasnitskaya, Moscow, 101000, Russia
[e] Department of Mathematics and Institute for Women's Health, University College London, Gower Street, London, WC1E 6BT, United Kingdom

ARTICLE INFO

Keywords:
Thermodynamics
Neuronal noise
Stochastic model
Sleep stage
Slow wave activity
Biophysical model

ABSTRACT

Although many models explain the spontaneous alternation between two distinct sleep states, Rapid Eye Movement (REM) and Non-Rapid Eye Movement (NREM), new empirical evidence has accumulated regarding consistent temperature changes during sleep stage transitions in small animals. The temperature dependence of neuro-excitability and low-frequency (≤4 Hz) neuronal activity has also been investigated theoretically and experimentally. Based on these phenomena, we constructed a stochastic thermodynamic model of the ultradian sleep rhythm. The model was validated through simulation, demonstrating statistical properties that align with experimental data from rats. This model would provide new insights into the mechanisms behind the REM cycle and can be applied in new therapies for sleep disorders.

1. Introduction

For most animals, it has been found that there are generally two behaviorally, metabolically, and electrophysiologically distinct states in sleep: Rapid Eye Moving (REM) state and Non-REM (NREM) state [1,2]. Representatively, slow wave activity (SWA), which is shown as a synchronized neuronal oscillation between depolarization ('UP' state) and hyperpolarization ('Down' state) from 0.5 Hz to 4.5 Hz, is the highest in NREM states and is significantly lowered and desynchronized in REM states [3]. The NREM and REM states alternate each other throughout sleep with distinct bodily state. However, the mechanism of the cycle remains unclear.

The regulation of a sleep cycle is finely tuned by the activity of several groups of neurons located in the basal forebrain, diencephalon and brainstem, as well as by circadian and homeostatic mechanisms [4,5]. The mechanism of periodicity of sleep has been mathematically investigated in depth. Representatively, the two process theory explains sleep and wake cycle with homeostatic rhythm, 'S', and external trigger, 'C', such as day light [6]. This model could simulate SWA dynamics that decreases over a sleep period and simulate disruption of sleep-wake cycle with desynchronized external signal and internal rhythm [7,8].

However, the objection to the theory of global homeostatic sleep has been suggested with empirical discovery of presence of local sleep. As well as the uni-hemispheric sleep of whales, predominance of SWA in local brain region has been observed in waking rodents with increasing rates of mistake in the task [9,10]. The increment of amplitude of delta wave (0.5 to 4 Hz) in the waking states was also found to be related to pathological states, and motivational and affective function [11]. Even in sleeping state, local SWA is more common than global SWA [9].

The function of SWA in NREM state is explained with restorative role, such as replenishment of glucose and brain waste clearance in astrocytic cells, which is shown with increasing risk of diabetes with reduction of NREM sleep [11]. SWA in sleep also negatively associates with sympathetic activity of cardiovascular activity and cortisol secretory rate [11]. High infra-slow oscillation in frequency under 0.1 Hz, one of characteristics of NREM sleep, are shown to be related to glial metabolism and autonomic regulation across gastric, cardiovascular and respiratory organ [12–15]. This strong association between autonomic regulation and slow wave sleep has been explained with the visceral theory that the sleeping state is switched into interoception toward visceral signal rather than the exteroception mainly active in waking state [16]. It was also empirically shown with synchronized response of visceral organ and cortex in NREM sleep, which was absent in REM sleep and waking state [17]. On the other hand, the function of REM state is understudied but might be to check the restorative process with memory recall in neural network strengthened with restored astrocytic network, called "dream" [18].

The source of delta wave in the waking and sleep states was found to be generally same, medial frontal cortex, although it is scattered

* Corresponding author at: Department of Mathematics and Institute for Women's Health, University College London, Gower Street, London, WC1E 6BT, United Kingdom.
E-mail address: alexey.zaikin@ucl.ac.uk (A. Zaikin).

https://doi.org/10.1016/j.chaos.2024.115732
Received 7 October 2024; Received in revised form 26 October 2024; Accepted 3 November 2024
Available online 20 November 2024

over frontal cortex [11]. It implies that SWA is locally originated from metabolic demand in occasional frequency during waking state and spreads out across global brain in the sleeping state [19].

The smallest unit that can sleep has been also suggested to consist of 7 to 8 neutrons and single astrocyte connected with the neurons [20]. Based on the restoration of glucose, glial energy source, during sleep, overconsumption of glucose may lead to abated astrocyte's potassium ion buffer, which is essential to maintain neural membrane potential [21]. It can induce local synchronization of slow wave activity through extracellular potassium ion diffusion into neighboring neurons after single neural activity. The neural coupling induced by extracellular potassium medium and neuronal noise simulated local SWA with synchronized depolarization and hyperpolarisation state of regional neurons [22].

Meanwhile, there has also been emerging evidence about a relationship between temperature and vigilance state transition [23]. Brain and core temperature is kept nearly constant due to homeostasis in the waking state, but in the sleeping state, thermoregulation is augmented. There are various fluctuations of temperature in the body in the range of about 1.5 °C [24]. Especially when the body goes from waking to sleeping, body temperature rapidly decreases due to vasodilation, and vice versa [23,25]. This correlation between body temperature and sleep-wake cycle has been modeled with temperature-dependent neuronal noise and applied in explanation for many neurological pathologies [26,27].

Furthermore, there is also a correlation between brain temperature and the REM cycle, which is more subtle and complicated than the correlations in the sleep-wake cycle. Typically, for small mammals, such as rodents, the transition into the NREM state accompanies decrement of brain temperature, and the transition from the NREM to the REM state accompanies an increment of brain temperature [28–32]. The relationship is reliable enough that brain temperature can be predicted by the sleep-wake state [33]. Brain temperature increment in REM state and decrement in NREM state was found in many homeotherms including birds [1]. This relationship also induced theories that brain warming is the function of REM against brain cooling in NREM state [1]. Although, for larger mammals, such as anthropoids including humans, there is no consistent polarity of brain temperature change in the transition of sleep state, which weakened the theories, within a single cycle, rates of brain temperature change in NREM is always smaller than those in REM [34]. While not having temperature change pattern of small homeotherms, poikilothermic animals, which have high variation of brain temperature, have the highest EEG power in delta band even in the waking state [11]. Furthermore, it has been shown that slight changes in temperature can have dramatic effect on sleep content in slow wave sleep; more specifically, half-a-degree increase in skin temperature was associated with an increase in slow wave sleep; and modulation of core temperature disrupted REM cycle pattern [35,36]. It is also known that humans have the highest portion of REM state around 4AM, when the body temperature is the lowest. Especially in the REM state, it shows a nonsynchronous relationship between body and brain temperature, which depends on ambient temperature [37]. It is supposed to be associated with peripheral vasoconstriction in REM state reduces volume of the core compartment of body [38–41].

In the neuronal level, resting membrane potential negatively correlates with temperature [42]. In addition, neuronal noise with frequency less than 2 Hz induced by the fluctuations of ion channels negatively associated with temperature due to shorter time constant in high temperature, which has been shown empirically and theoretically [43,44].

Brain cooling was suggested to be one of the function of NREM state with correlation of amount of NREM portion with heat from exercise in the waking state, with theory that slow wave sleep decreases the body and brain temperature [45]. Some theories about brain warming in REM state suggested increment of cerebral blood flow and others suggested increment of neuronal activity in REM state as a cause of brain temperature change with sleep stage transition [1]. The former theories explained that the brain temperature change with increased heat transfer from the core body via blood flow. However, it was objected with the empirical evidence that core temperature is always lower than brain temperature [46,47]. This led to the other theory that increased neuronal activity in REM state drives increment of brain temperature [46,48]. However, the higher brain activity in REM state had not been experimentally verified.

The standard biological model to explain the NREM–REM cycle is the reciprocal interaction model. The REM state is driven by reciprocal inhibition of REM-on cells and REM-off cells [49]. It has been simulated with a mathematical model with Lotka and Volterra equations and successfully reproduced unit activity of REM-on and REM-off cells experimentally acquired, which gave verification of the biological model [50]. It has also been simulated with a mean-field model considering voltage fluctuations and state-dependent connectivities, which are found to change with switching on REM-on or REM-off cells [49,51]. The model showed first-order phase transition between REM and NREM state [51]. As illustrated in these examples, mathematical models can help, under a few assumptions, inferring the roles of different parameters in a given system, such as the ultradian sleep rhythm. However, these models are yet to reflect recent empirical discovery on local SWA and temperature-association of REM–NREM transition.

Based on the empirical evidence above, we suggest a model to explain the REM cycle with thermodynamics in the sleeping brain. For simplicity of the model, we made these assumptions and approximations for the model.

- Spontaneous neuronal firing induced by neuronal noise is the only neuronal activity in sleep.
- Heat transfers via heat conduction from the scalp into the room and heat advection from the brain to the body for thermoregulatory process in sleep, neglecting core and brain temperature change with circadian rhythm. It will be treated in the later part of this paper.
- Neurons of the neocortex are regularly embedded in a half-sphere-shell, globally sharing extracellular potassium medium.

To simulate the bodily thermodynamics, we constructed thermoregulatory model with segments of brain and body with heat generation from neuronal firing and passive heat transfer. Many mathematical formulation of thermoregulation has incorporated model with multi-segments and multi-nodes [52]. One of them successfully simulated body temperature decrements with protocols of therapeutic hypothermia to prevent hyperthermia due to inflammation in post-cardiac patients [53]. This network based viewpoint to analyze the interaction within body or organ facilitates simpler quantification and formulation of complex physiology in living system [54].

This paper is structured as followings. In the second section, we describe the model's outline and construct the model from the beginning, the derivation of the stochastic SWA of the model, and sequentially develop the model into the form previewed in the outline. In the third section, the method and result of verification of the model with empirical data analysis and computational simulation will be given, and two additional demonstrations from the model will be demonstrated in the fourth section. We will discuss the limitations, and implications in the fifth section.

2. Construction of the model

In the model, the brain is the system, and the neocortex is a region of interest, which is the main organ for SWA [55]. The room where the one is sleeping is assumed as the heat reservoir with a constant temperature. The body is connected to the system with a constant temperature gap in the NREM state [47,56], while it is thermally disconnected from the system in the REM state based on the discrepancy of thermal

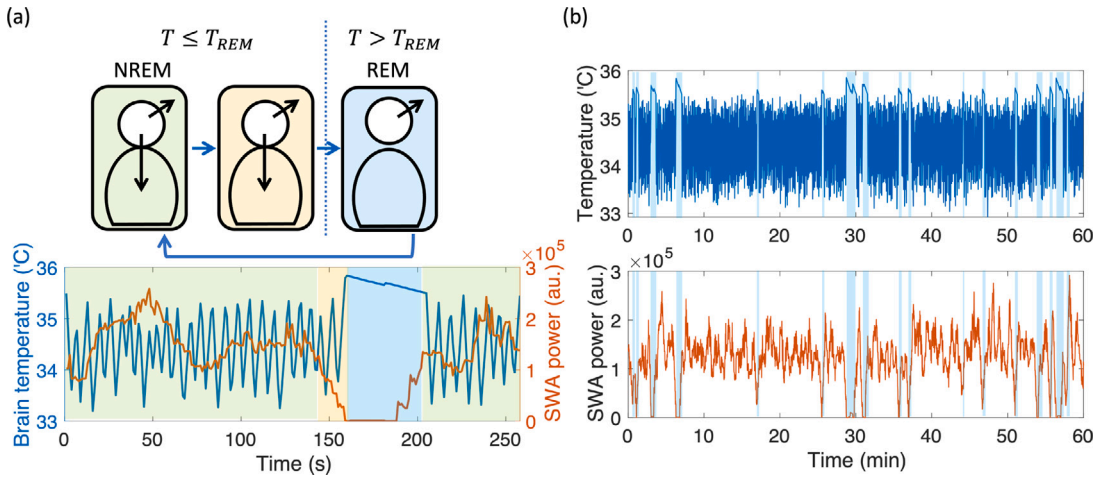

Fig. 1. Concept of the model. (a) The main concept of the model (top) and plot (bottom) for brain temperature (blue line in bottom panel) and SWA power (orange line in bottom panel) during a cycle. First, in the NREM state, the brain emits heat within the body and into the air, and its temperature decreases (green shades). At the same time, heat generation from SWA in the brain increases, and temperature increases over the threshold of the REM state (yellow shades). Third, in high temperature of the REM state, neural heat generation decreases, but heat dissipation into the body decreased (blue shades). Temperature decreases again, and it goes back into the first stage.(b) Simulated brain temperature (top) and SWA power (bottom) in a series of REM cycles in 60 min. REM state is marked with blue shades. ζ = 1.4258 °C/s and γ = 8.5659e−04 °C/s are used as heat transfer parameters in simulation of (a) and (b).

response in brain and core in the state [37,38]. The model is briefly described in Fig. 1 (a). In the NREM state, the brain dissipates heat into the core through advection and the room through conduction. It decreases brain temperature (green shade) and increases the probability of SWA because lower brain temperature increases neuronal excitability to generate SWA. Neural heat caused from SWA stochastically increases the brain temperature. If it goes over the threshold of the REM state (yellow shade), the brain-body gets thermally disconnected from the body, as an approximation for the peripheral vasoconstriction [39,40], and dissipates heat exclusively into the room. It makes temperature rise in the REM state despite the low SWA. However, low SWA in the REM state stochastically induces brain temperature to drop again (blue shade), and the brain goes back into the NREM state. Figure 1 (b) displays simulation results of time series of stochastic REM cycles, showing oscillating brain temperature and SWA power with the cycles.

First, the stochastic variable of heat generation from SWA is simulated with local SWA model with temperature dependence. Next, the heat generation is combined with heat dissipation to get differential equation of brain temperature. The symbols and corresponding values to be used in Eq. (1) to (14) and the simulation is in Table 1.

The simulation of SWA is based on Postnov's model with stochastic differential equations on membrane potential of neuron i, V_i, in the set of neurons and neuronal noise [22]. The temperature dependent neuronal current for thermal variation of membrane potential, I_T, was added to the formula with potassium, sodium, leakage current, $I_{i,K}, I_{i,Na}, I_{i,L}$ in Eq. (1). The model is based on Leech P-neuron's parameters on Table 1, and Eq. (2), (3), (4), and (5) on $I_{i,K}, I_{i,Na}, I_{i,L}$, and Eqs. (8) and (9) on potassium equilibrium potential $[K]_0$ and extracellular potassium concentration $[K]$ are from the Postnov et al. 2007. It assumes system of neurons and extracellular potassium medium connected with reservoir of potassium ions with $[K]_0$, preventing biologically implausible sustained accumulation of potassium ions in extracellular medium. It simulates SWA with coupling of neurons via extracellular potassium ions and neuronal noise facilitating collective firing.

$$C_m \frac{\partial V_i}{\partial t} = -I_{i,K} - I_{i,Na} - I_{i,L} + I_{i,app} - I_T \tag{1}$$

$$I_{i,K} = g_K n_i^N (V_i - E_{i,K}) \tag{2}$$

$$I_{i,Na} = g_{Na} m_i^M h_i^H (V_i - E_{Na}) \tag{3}$$

$$I_{i,L} = g_L (V_i - E_L) \tag{4}$$

$$I_{i,app} = I_{app0} + \sqrt{D}\xi_i(t) \tag{5}$$

$$I_T = \beta(T - T_0) \tag{6}$$

$$V_{i,K} = \frac{RT}{F} \ln \frac{[K]}{[K]_i} \tag{7}$$

$$W \frac{\partial [K]}{\partial t} = \frac{1}{F} \Sigma I_{i,K} + \gamma([K]_0 - [K]) \tag{8}$$

For the parameters for activation variables in Eq. (9), the values suggested for α_κ and β_κ in Postnov et al. 2006 were used. The Q factors of time constant Q_κ that variates the kinetic rates of ion channels about temperature in Eq. (10), where $\kappa = n_i, m_i, h_i$, slow down voltage variation in action potential in lower temperature. It was empirically shown in vitro and in vivo neurons and facilitate in collective firing in lower temperature [42,59]. With I_T in Eq. (6) that gives linearly decreasing resting membrane potential with increasing brain temperature, the firing rates of the SWA model exponentially decay with increasing temperature, as shown in Fig. 2 (a).

$$\frac{\partial \kappa}{\partial t} = \frac{\alpha_\kappa(1-\kappa) - \beta_\kappa \kappa}{Q_j} \tag{9}$$

$$Q_\kappa(T) = A_\kappa^{-\frac{(T-37)}{5}} \tag{10}$$

The firing rate $R(t)$ is converted into the rate of heat generation from ATP after the firing as shown in Eq. (11). The heat from ATP after single firing g is calculated based on simulation of local SWA model with Eq. (12), which calculates 25% of free energy of ATP to return sodium concentration to equilibrium after action potential. The rate of 25% has been suggested as the ratio of heat dissipation of ATP to the total free energy of ATP during action potential in multiple literatures [60,61]. The heat generation during action potential due to ATPase in membrane was also empirically verified with in vitro nerves [62,63].

$$q(t) = gNR(t) \tag{11}$$

$$g = \frac{\lambda}{4} \int g_{Na} m^M h^H (E_{Na} - V_i) dt \tag{12}$$

Then, the heat generation rate $q(t)$ is combined with the heat dissipation rates, ζ and γ, to make out stochastic differential equation

Table 1
Value of fixed parameter.

Symbol	Meaning	Value	Unit
T_0	Standard brain temperature for linear temperature dependence.	35	°C
T_a	Ambient temperature	25	°C
C_m	Neuronal membrane capacitance in Leech P-neuron model	1	μF/cm^2
g_K	Conductance of neuronal potassium current	6	mS/cm^2
g_{Na}	Conductance of neuronal sodium current	350	mS/cm^2
g_L	Conductance of neuronal leakage current	350	mS/cm^2
E_{Na}	Equilibrium potential of neuronal sodium current	60.5	mV
E_L	Equilibrium potential of neuronal leakage current	49	mV
β	Negative Linear correlation between temperature and resting membrane potential [42].	−10	mV/°C s
N	Activation subunits of neuronal potassium channel	2	
M	Activation subunits of neuronal sodium channel	4	
H	Inactivation subunits of neuronal sodium channel	1	
A_K	Q factor of potassium channel	2.3	
A_{Na}	Q factor of sodium channel	3	
I_{app0}	Neuronal injection current	12.2	μA/cm^2
D	Variance of neuronal injection current noise	2700	μA^2/cm^4
W	Extracellular volume per unit area of cell surface	0.5	nl/cm^2
$[K]_0$	Equilibrium extracellular potassium concentration	4	mM
N	Number of neurons in neocortex [57].	2.1e7	
g	Emission of thermal energy from ATP during single action potential	1.3529e−08	J
λ	Energy supplied by a molecule of ATP during action potential	4.9834e−20	J
$T - T_{core}$	Difference between brain temperature and core temperature in thermoregulation [47].	0.5	°C
T_{REM}	Lower threshold for brain temperature of REM state	35.5	°C
T_a	Ambient temperature of the room	25	°C
C_{brain}	Heat capacity of brain [58].	6.5340	J/°C

of brain temperature. Eq. (13) is for the brain temperature variation in NREM state, and Eq. (14) is for the brain temperature variation in REM state, where T is brain temperature, T_{core} is core temperature, and T_a is ambient temperature of the room; ζ is the rates of temperature change through heat transfer to the body, heat advection rate; and γ is the rates of temperature change through heat transfer to the room, which is heat reservoir, heat conduction rate. As explained above, $T - T_{body}$ and T_a are constant parameters because room is heat reservoir with T_a, and in NREM state, brain and body are thermally connected with constant gradient.

$$C_{brain}\frac{\partial T}{\partial t} = -C_{brain}(\zeta(T - T_{body}) + \gamma(T - T_a)) + q(T).\ (T \le T_{REM}) \quad (13)$$

$$C_{brain}\frac{\partial T}{\partial t} = -C_{brain}\gamma(T - T_a) + q(T).\ (T > T_{REM}) \quad (14)$$

As Fig. 2(a) shows, the stochastic heat generation and the deterministic heat generation in NREM and REM state have different stable points with high mean firing rate in low temperature and low mean firing rate in high temperature, respectively. The firing rate is close to Poissonian variables with standard deviation of firing rates close to the mean firing rates in the temperature. The stochasticity of heat generation from noise-induced firing allows the transition of the sleeping state from NREM to REM state and from REM to NREM state.

While other all parameters are fixed, parameters for heat advection rate ζ and heat conduction rate γ are main control parameters. The diagram in Fig. 2(b) shows the regimes of sleep state dynamics with different ζ and γ. First, when γ is too small, the transition from REM to NREM state is suppressed, making the regime 'REM-predominant'. Conversely, when γ is too high, the duration of REM state becomes very short because stable point in REM state has lower brain temperature than the threshold temperature T_1, making the regime 'NREM-predominant'. In other words, γ is negatively associated with duration of REM duration. Second, when ζ is too small, stable point in NREM has low firing rate, so the probability of the transition from NREM to REM state is rare. When ζ is too high, with high firing rate, the transition from NREM to REM is frequent. In other words, ζ can be said to modulate the instance of REM state, or period of REM cycle with negative association. Only the regime of gray color in Fig. 2(b) has stable REM cycle with intermediate periods.

3. Verification of the model

3.1. Method of data analysis and simulation

We drew on Petersen et al.'s recent dataset of rats' local field potential (LFP), brain temperature, and sleep scores for every second [64,65]. Adult male Long-Evans rats with 250–450 g, aged three to six month old, were used. The rats' LFP is measured in their bilateral hippocampus with 1250 Hz of sampling rates for two to twenty-four hours of sessions, and their brain temperature is measured in their hippocampus. The sleep score is classified into one stage among 'WAKE,' 'NREM,' 'Intermediate,' and 'REM' with automatic sleep scoring [66]. It used three features for sleep scoring: the first principal component of the electrophysiological signal (PC1), electromyogram (EMG), and theta wave. The 'NREM' state has high PC1, intermediate EMG, and low theta wave; the 'REM' state has low PC1, low EMG, and high theta wave; and the 'WAKE' state has low PC1, high EMG, and low theta wave [66].

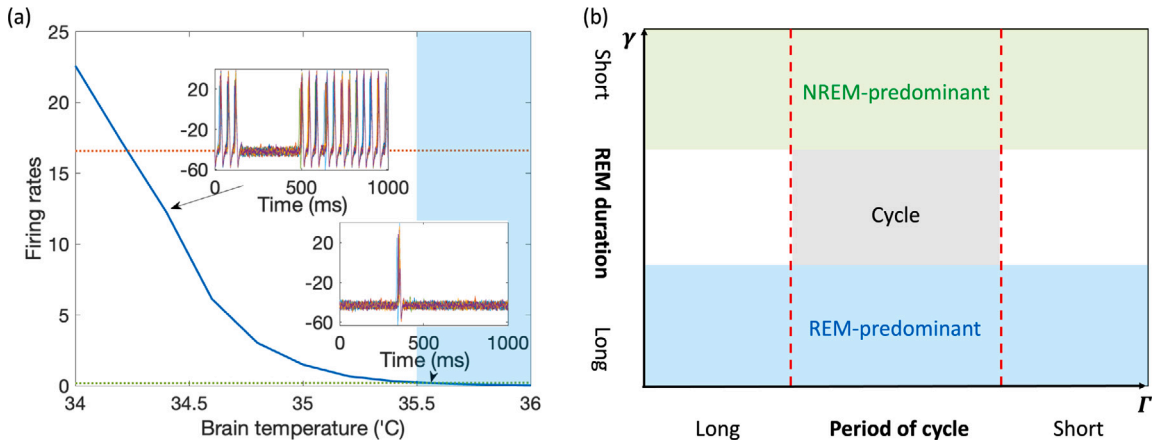

Fig. 2. (a) Mean firing rates with varying brain temperatures (blue line). The intersection of blue line with orange dotted line is firing rate of steady state in NREM state, and the green dotted line is for the REM state. The blue shade marks the region of temperature over threshold of REM state in the model. The small insets shows time series of membrane potentials of neurons in the brain temperature 34.4 °C (left) and 35.6 °C (right) with millivolts of y-axes. The mean firing rates exponentially decrease with increment of temperature. $\zeta = 1.4258$ °C/s and $\gamma = 8.5659e{-}04$ °C/s are used as heat transfer parameters in the simulation.(b) Diagram of the regimes on the parameter for heat advection rate ζ and heat conduction rate γ regulating period of cycle and REM state duration, respectively. Green and blue shade mark 'NREM-predominant' regime and 'REM-predominant' regime, respectively, and the regime between them has stable REM cycle. The regime between two red dotted lines have the intermediate period of REM cycle. The gray regime has stable REM cycle with intermediate period. (For interpretation of the references to color in this figure legend, the reader is referred to the web version of this article.)

We used nine rats' data (MS12, MS13, MS21, MS22, TEMP R04, TEMP R05, TEMP R07, TEMP R08, TEMP R09) among ten rats' data and excluded temperature-modulating range following related data given in the sets. Also, the 'WAKE' sleep state is additionally classified into 'WAKE' meaning long-term waking, and 'Micro Arousal' meaning short-term waking following the standard in B. O. Watson et al.'s paper [66]. For the data we analyzed, the 'WAKE' state is excluded because the model is only for sleeping states, and the 'MicroArousal' state is included because the state is generally included in sleeping states. We concatenated multiple sessions within a single animal, not to put weight on the number of sessions in each animal. To get the power of SWA, each animal's LFP was Fourier transformed in overlapping time windows of 20 s with 19 s of overlaps, and the power of signals in the frequency range from 0.5 Hz to 4 Hz was summated in each time window to make out time series SWA data.

Heat transfer parameters γ and ζ are fitted with data because the heat transfer rate within the body is challenging to measure empirically. Simulation of membrane potential V_i was done using 0.1 ms of time bin and fourth order Runge–Kutta for 5 h of simulation times, 5 x 3600 x 10000 time bins. The firing rates $R(t)$, heat generation rate $q(t)$, applied current $I_{i,app}(t)$, and temperature dependent current $I_{i,T}$ were acquired in every second, or 10000 time bins. The summation of membrane potential of all neurons V_i was converted into power spectral density, and the power of SWA in 0.5 to 4 Hz was acquired with same length of time window and same length of overlaps with empirical data analysis. In the model, the REM state is defined as the state with temperature over than T_{REM}, and the NREM state is the state that is not REM state, while for experimental data, sleep score, 'NREM' and 'intermediate state' was classified into the NREM state, and 'REM' was classified into REM state, which were given for each second of the data.

Cumulative probability of normalized duration of SWA burst $P(\frac{d_{SWA}}{<d_{SWA}>} > x)$ in data is used to fit the parameters, which has been suggested as a robust statistical property of sleeping states. It is adjusted to be the magnitude of SWA over threshold voltage due to the absence of theta wave in the model [67]. The threshold of the SWA burst is set to the median value of time series of the SWA power in each animal. $P(\frac{d_{SWA}}{<d_{SWA}>} > x)$ of each animal is separately analyzed, and interquartile range and median value across all animals were acquired as the blue shades and data points of circle in Fig. 3(a) and (b). The cumulative probability of SWA burst of simulation is acquired with same method with empirical data analysis. For validation data, cumulative probability of REM duration was used. For reliable statistical analysis, six animals (MS12, MS13, MS22, R07, R08, R09), which have instances of REM state over ten, were used for the analysis of cumulative probability.

Maximum Likelihood Estimation was used to estimate fitness for each set of parameters of γ and ζ. With the model using each set of parameters, the simulation generated the cumulative probabilities for eight data points. Probabilistic likelihood $P(y_i|\theta) = \prod_i P(y_i|\theta)$ was acquired for each set of parameters with Monte-Carlo method where θ is the set of parameters γ and ζ, and $P(y_i|\theta)$ is probability for the simulated cumulative probability with the parameters to be in 95% confidence interval of median value of the cumulative probability of data at the data point. The 95% confidence interval is acquired with the method suggested by R. McGill [68]. The optimal set of parameters is $\theta = \underset{\theta}{argmax}(\log_{10} P(y_i|\theta))$. Then, we assessed predictive validity with the parameters-fitted model, generating other statistical properties and comparing it with one of the data. The other parameters are fixed parameters that are generally drawn on from the results of empirical research, as Table 1 about parameters shows.

3.2. Verification of the model

With the method suggested above, the model parameters were fitted, and it was tested to see if it could reproduce another statistical property, the cumulative probability of the normalized duration of the REM state. Fig. 3 shows parameter fitting and testing for the model. As explained in the Method section, the parameters of the model are set to parameters with maximum likelihood to give the cumulative probability of data for the normalized duration of SWA burst, which are $\zeta = 1.4258$ °C/s and $\gamma = 8.5659e{-}04$ °C/s as in Fig. 3(a). We used these parameters for all of the following results. With the parameters, we generated a simulation result of the normalized duration of the REM state. Fig. 3(b) shows it agrees relatively well with experimental data, under consideration that the number of REM duration in empirical data is limited for reliable statistical analysis. The model with parameters fitted with the SWA burst data can reproduce cumulative probability of the normalized REM duration in data. Beyond statistical property of normalized value, as in Fig. 3(c) of empirical time series of SWA power shows, the period of rat's REM–NREM cycle is few minutes scale, and the simulation result in Fig. 3(d) agrees well for the point as well [69].

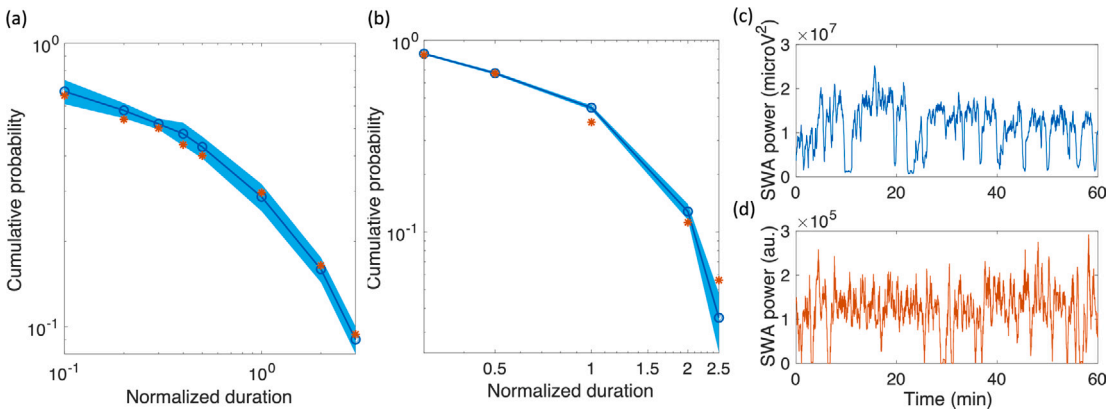

Fig. 3. Parameter fitting and testing for the model. (a) Cumulative probability for the normalized duration of SWA burst of data and simulation with fitted heat transfer parameters. Median values of cumulative probability of data (blue line) with 95% confidence interval of the median values (light blue shade) are overlapped with values of cumulative probability of simulation (orange star). The simulation parameters set of ζ = 1.4258 °C/s and γ = 8.5659e−04 °C/s had maximum likelihood (0.875) for the normalized duration of the SWA burst in data among sets of parameters. (b) Cumulative probability for the normalized duration of REM state of data and simulation with parameters in (a). Median values of cumulative probability of data (blue line) with 95% confidence interval of the median values (light blue shade) are overlapped with values of cumulative probability of simulation (orange star). The simulation of the model fitted with the empirical SWA power can reproduce REM durations close to those of data. (c) Representative empirical time series of SWA power of a rat for 60 min. (d) Representative simulation of SWA power with the parameter fitted in (a) for 60 min. The time scale of SWA power dynamics is similar to the data in (c).

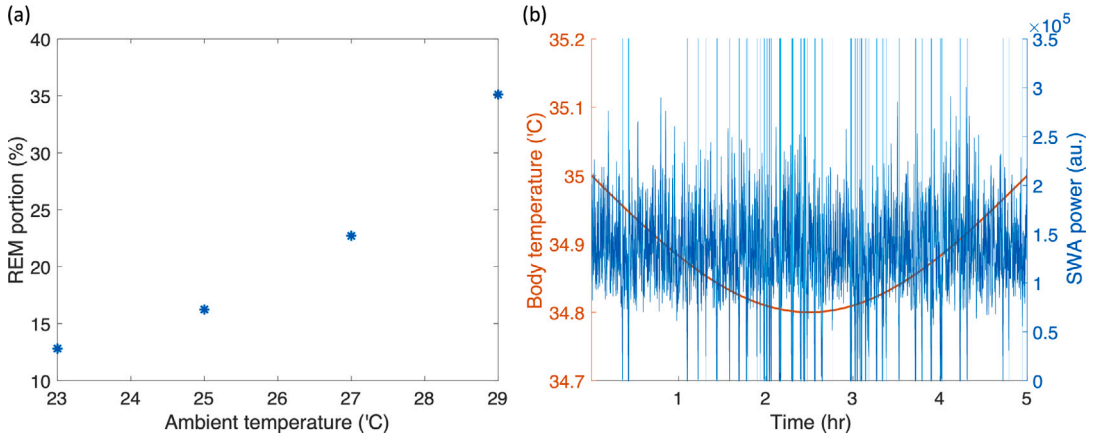

Fig. 4. (a) Change of the REM portion depending on ambient temperature (23, 25, 27, 29 °C). REM state portions increase with increment of ambient temperature. (b) Hypnogram (blue line) of the simulation of the model with consideration of the change of the circadian core temperature. The light blue shades show the REM state. In the nadir of body temperature, around 2-3 h after onset of sleep, the simulation shows highest propensity to REM state. ζ = 1.4258 °C/s and γ = 8.5659e−04 °C/s are used in simulation of (a) and (b).

4. Demonstration of other characteristics of REM cycle with the model

This model can also generate other phenomena of rats' sleep with the change of specific parameters. First, we will show that it can generate some sleep phenomena discovered in previous empirical research with the following results. Fig. 4(a) shows that simulation reproduces general trends of REM portion change in the total simulation period depending on ambient temperature discovered in empirical literature [70]. According to the literature, rats' REM portion of sleep significantly increases when ambient temperature increases. At 22 degrees Celsius of ambient temperature, 88.6% of the rat's total sleep was in the NREM state, but at 29 degrees Celsius, 86.3% of the rat's total sleep was in the REM state. We tried simulation with all other parameters the same as previous simulations, but various ambient temperatures T_a from 22 to 29 degrees Celsius. Though the simulation result did not give the same number for the REM portion — 12.8% of REM and 87.2% of NREM at 21 °C, and 35.1% of REM and 64.9% of NREM at 29 °C, it reproduced overall trends of REM portion change that increases with ambient temperature increases.

In contrast to human circadian rhythm with highest body temperature in noon and the lowest in the midnight, rodents have their lowest body temperature in the noon and the maximum body temperature in the midnight [71]. However, rodents and humans commonly have the highest propensity to REM state in time with the lowest body temperature [72]. Up to this point, the effect of circadian rhythm was excluded for simplicity, but to see if the model can reproduce the effect of body temperature variation, the sinusoidal variation of body temperature of 0.2 °C is added to the model. In Fig. 4(b), with body temperature minimizing at 2.5 h (orange line), we can see the REM portion (blue shade) increasing around the minimal point of body temperature. Even with opposite circadian rhythm across species, humans and rodents have same relationship between pattern of REM portion and body temperature, which implies the robust association between REM cycle and body temperature, and it can be simulated with this thermodynamic model.

Also, Human has longer duration of REM state and period of REM cycle with tens of minutes than the rats used in this paper. It can be explained with lower ratio of heat dissipation rates to heat generation rate. As aforementioned, Fig. 2(b) shows that γ and ζ decide the length of REM duration and cycle period respectively. While the rodents would have higher ratio of γ and ζ to $q(t)$ to have the shorter lengths, human would have lower ratio, which can be explained with lower ratio of body surface to volume.

5. Discussion

Collective spontaneous neuronal activity of slow wave activity increases with decreasing temperature due to slower dynamics of action potential and hypo-polarized resting membrane potential. The heat induced from slow wave activity can increase brain temperature. The association between slow wave activity and temperature can be the principle of the NREM–REM cycle. We suggested the model to explain the mechanism of the NREM and REM cycle with thermodynamics and temperature-dependent neuronal states. The model considers generation of local SWA from neuronal noise, heat generation from neuronal activation, and heat dissipation from the brain to the core and air for thermoregulation. The model also considers the breakage of core thermoregulation in the REM state with disconnection of thermal contact between the brain and core. Two stochastic differential equations for REM and NREM states describe brain temperature change with stochastic heat generation and deterministic heat dissipation, simulating the spontaneous REM–NREM cycle.

The model was parameter-fitted with the probabilistic distribution of duration of SWA bursts, and it was validated with the prediction of probabilistic distribution of duration of REM states, which is distinct property from SWA burst. Then, other phenomena about the cycle of sleep stage were demonstrated with the model: Change of REM portion with different ambient temperature and varying pattern of REM cycle riding on circadian rhythm. In this section, we will discuss the limitation of the research, the bespoken point in the Results section, and the consistency of this model with other precedented research.

However, there are several limitations in the research. First, there is a limitation of physiological reality in the model. It did not include a physiologically plausible response function in heat diffusion and extracellular ion concentration but assumed heat diffusion from the brain to the body in a second and instant equilibrium of extracellular medium concentration. Also, without consideration of spatial heterogeneity of neural distribution and extracellular potassium concentration, local SWA model is applied on global brain situation. Despite the simplicity, the model could reproduce the statistical property of the REM cycle, which might imply that it includes the core of the mechanism. However, the delay in heat diffusion and reaching heat equilibrium might explain the species-dependent difference of temperature correlation in the sleep stage transition. Compared with rodents, which show evident temperature change, primates, which have bigger brains and bodies than rats' brains and bodies, have a weaker temperature correlation with sleep stage transition. The model considering response time for heat diffusion from neuronal activity should be investigated further.

Second, the reduction of heat transfer from the brain to the body in the REM state assumed in this model is not verified empirically. However, it was assumed based on discovery of peripheral vasoconstriction in REM state. The difficulty of measuring heat transfer in the body and in real-time would prevent us from exploring this possibility empirically, and it could be indirectly verified with this computational simulation.

Lastly, the model is under the assumption that the body is a passive system in thermodynamic interaction with the environment for simplification. It only switches the REM state on and off with brain temperature. However, bodily thermodynamics is an active and more complex system beyond the assumption of temperature-dependent neuronal noise and thermodynamics. Especially the hypothalamus is known to actively modulate bodily state to be in preferable temperature, which is explained by the active process of homeostasis or allostasis [73,74]. This oversimplification of this model would explain the discrepancy between the simulation and the data.

This model can seem to be in contradiction with the sleep-wake cycle model based on temperature-dependent neuronal noise. The sleep-wake cycle model suggests that low core temperature induces high neuronal noise in wake-promoting neurons to increase the propensity to the brief waking state, which is called the 'microarousal' state [27]. Then, high core temperature induces low neuronal noise in wake-promoting neurons, facilitating a lower frequency of waking and deeper sleep, which is also validated with experiments [27]. On the other hand, in our model, in low brain temperature, the NREM state, in other words, 'deep sleep,' is promoted, and the promoted NREM state also triggers high brain temperature and REM state, making the cycle spontaneous. It might seem contradictory with the previous theory. However, the core temperature in Dvir's paper is the mean temperature over the entire sleep period [27]. On the contrary, the brain temperature in our model is an instantaneous temperature for each time step, and it is unsynchronized with the core temperature in the REM state. Also, as mentioned with Fig. 4(b), when the mean body temperature is the lowest, the REM portion is the highest in the model. In the REM state, the short term waking state, microarousal state, is more frequent than in the NREM state, so the result agrees that low body temperature trigger wake-promoting cells. [75]. In addition, Fig. 4(a) shows that high ambient temperature induces a sustained state in REM state, which is the same conclusion as Dvir's paper in 2018. Therefore, our model is consistent with conclusion of Dvir's model.

In empirical research to monitor cortical and hypothalamic temperature in the transition of vigilance state, it was found that for sleep-wake transition, hypothalamic temperature change precedes cortical temperature change, while for NREM–REM transition, cortical temperature change precedes hypothalamic cortical temperature change. It was discussed to support the suggestion that the neocortex dominantly leads temperature change in the NREM–REM transition, and the hypothalamus dominantly leads temperature change in the sleep-wake transition in the paper, which supports separated circuits for sleep-wake cycle and NREM–REM cycle [31]. This suggestion is also consistent with our model that brain temperature change across NREM and REM states is explained by neuronal activity in the cortical cortex.

The results of simulation on this thermodynamic model of REM–NREM cycle imply strong association of brain temperature change with the oscillation of sleep stage. However, it is unclear if the brain temperature change drives the cycle or the sleep stage transition induces the brain temperature change. Many previous brain warming and cooling theories suggests that NREM sleep decreases the brain temperature with lower metabolic demands, and brain in REM state increase temperature with increased neuronal activity, stating thermoregulation function of REM cycle [1,45]. On the other hand, in this model, brain does not actively regulate temperature, but the influence is bidirectional: brain temperature induces neuronal activity of NREM state, and the neuronal activity warm up the brain. The advantage of bidirectional regulation over one-directional regulation is the energy efficiency of the REM cycle. The existence of the effect from brain temperature to sleep stage cycle can be implied by many experiments that ambient or body temperature modulation also affects sleep stage pattern [35,36]. For direct evidence to know if brain temperature induces transition of sleep stage, delay in coupling between temperature and sleep stage phases can be analyzed from experimental data. It can show if temperature change precedes transition from NREM to REM state and from REM to NREM, although it should be considered that the time resolution of delay would be limited by the low frequency of SWA.

In this research, we suggested a thermodynamic model to explain the mechanism of the REM cycle. This model has successfully reproduced the REM cycle with merely thermodynamical processes. The model can be contribute in many research to enhance sleep quality. Interdependence between thermoregulation and sleep-related disorders such as insomnia can be investigated further in new perspectives [76]. It can contribute to development of treatment using temperature control for better quality of sleep in insomnia patients, which is being actively studied in medical engineering [35]. Also, the model may be the base to understand the change of REM and NREM phase pattern in babies with relation to weaker thermo-regulation [77].

CRediT authorship contribution statement

Haeun Sun: Writing – original draft, Validation, Methodology, Investigation, Formal analysis, Data curation, Conceptualization. **Yurii Ishbulatov:** Writing – review & editing. **Anatoly Karavaev:** Writing – review & editing. **Denis Zakharov:** Writing – review & editing. **Alexey Zaikin:** Writing – review & editing, Supervision.

Declaration of competing interest

The authors declare that they have no known competing financial interests or personal relationships that could have appeared to influence the work reported in this paper.

Acknowledgments

AZ is supported by a Medical Research Council, United Kingdom grant (MR/R02524X/1). DZ, AZ acknowledge the Basic Research Program at the National Research University Higher School of Economics (HSE University) and its HPC facilities, Moscow, Russia.

Data availability

Data will be made available on request.

References

[1] Ungurean G, Barrillot B, Gonzalez DM, Libourel PA, Rattenborg NC. Comparative perspectives that challenge brain warming as the primary function of REM sleep. iScience 2020;23(11):101696. http://dx.doi.org/10.1016/j.isci.2020.101696.
[2] Fiorillo L, Puiatti A, Papandrea M, Ratti P-L, Favaro P, Roth C, et al. Automated sleep scoring: A review of the latest approaches. Sleep Med Rev 2019;48:101204. http://dx.doi.org/10.1016/j.smrv.2019.07.007.
[3] Adamantidis AR, Herrera CG, Gent TC. Oscillating circuitries in the sleeping brain. Nat Rev Neurosci 2019;20(12):746–62. http://dx.doi.org/10.1038/s41583-019-0223-4.
[4] Peever J, Fuller PM. The biology of REM sleep. Curr Biol 2017;27(22):1237–48. http://dx.doi.org/10.1016/j.cub.2017.10.026.
[5] Eban-Roghschild A, Appelbaum L, de Lecea L. Neuronal mechanisms for sleep/wake regulation and modulatory drive. Neuropsychopharmacology 2018;43(5):937–52. http://dx.doi.org/10.1038/npp.2017.294.
[6] Borbély AA, Daan S, Wirz-Justice A, Deboer T. The two-process model of sleep regulation: a reappraisal. J Sleep Res 2016;25(2):131–43. http://dx.doi.org/10.1111/jsr.12371.
[7] Achermann P, Dijk D-J, Brunner DP, Borbély AA. A model of human sleep homeostasis based on EEG slow-wave activity: quantitative comparison of data and simulations. Brain Res Bull 1993;31(1–2):97–113. http://dx.doi.org/10.1016/0361-9230(93)90016-5.
[8] Postnov DE, Merkulova KO, Postnova S. Desynchrony and synchronisation underpinning sleep–wake cycles. Eur Phys J Plus 2021;136:597. http://dx.doi.org/10.1140/epjp/s13360-021-01491-z.
[9] Nir Y, Staba RJ, Andrillon T, Vyazovskiy VV, Cirelli C, Fried I, et al. Regional slow waves and spindles in human sleep. Neuron 2011;70(1):153–69. http://dx.doi.org/10.1016/j.neuron.2011.02.043.
[10] Vyazovskiy VV, Olcese U, Hanlon EC, Nir Y, Cirelli C, Tononi G. Local sleep in awake rats. Nature 2011;472(7344):443–7. http://dx.doi.org/10.1038/nature10009.
[11] Knyazev GG. EEG delta oscillations as a correlate of basic homeostatic and motivational processes. Neurosci Biobehav Rev 2012;36:677–95. http://dx.doi.org/10.1016/j.neubiorev.2011.10.002.
[12] Lőrincz ML, Geall F, Bao Y, Crunelli V, Hughes SW. ATP-dependent infra-slow (<0.1 Hz) oscillations in thalamic networks. PLoS One 2009;4:e4447. http://dx.doi.org/10.1371/journal.pone.0004447.
[13] Vandenhouten R, Lambertz M, Langhorst P, Grebe R. Nonstationary time-series analysis applied to investigation of brainstem system dynamics. IEEE Trans Biomed Eng 2000;47:729–37. http://dx.doi.org/10.1109/10.844220.
[14] Lambertz M, Langhorst P. Simultaneous changes of rhythmic organization in brainstem neurons, respiration, cardiovascular system and EEG between 0.05 Hz and 0.5 Hz. J Auton Nerv Syst 1998;68:58–77. http://dx.doi.org/10.1016/s0165-1838(97)00126-4.
[15] Karavaev AS, Kiselev AR, Runnova AE, Zhuravlev MO, Borovkova EI, Prokhorov MD, et al. Synchronization of infra-slow oscillations of brain potentials with respiration. Chaos 2018;28:106309. http://dx.doi.org/10.1063/1.5046758.
[16] Morchiladze MM, Silagadze TK, Silagadze ZK. Visceral theory of sleep and origins of mental disorders. Med Hypotheses 2018;120:22–7. http://dx.doi.org/10.1016/j.mehy.2018.07.023.
[17] Pigarev IN. The visceral theory of sleep. Neurosci Behav Physiol 2014;44(4):421–34. http://dx.doi.org/10.1007/s11055-014-9928-z.
[18] Satori M. Simulating REM sleep in an in silico neuron-astrocyte network. (Master's thesis), London: University College London; 2022.
[19] Vyazovskiy VV, Harris KD. Sleep and the single neuron: the role of global slow oscillations in individual cell rest. Nat Rev Neurosci 2013;14(6):443–51. http://dx.doi.org/10.1038/nrn3494.
[20] Postnov DE. Spatiotemporal sleep dynamics and neurogliavascular unit signaling: Recent evidence calls for a new paradigm. In: Presented at the iComplex system and future technologies in neuroscience, Saratov, Russia. 2024, CSFTN-24-L11. https://www.sgu.ru/sites/default/files/page/files/csftn-24-l11.pdf.
[21] O'Donnell J, Ding F, Nedergaard M. Distinct functional states of astrocytes during sleep and wakefulness: Is norepinephrine the master regulator? Curr Sleep Med Rep 2015;1:2186. http://dx.doi.org/10.1038/s41467-023-37974-z.
[22] Postnov DE, Ryazanova LS, Zhirin RA, Mosekilde E, Sosnovtseva OV. Noise controlled synchronization in potassium coupled neural models. Int J Neural Syst 2007;17:105–13. http://dx.doi.org/10.1142/S012906570700097X.
[23] Harding EC, Franks NP, Wisden W. The temperature dependence of sleep. Front Neurosci 2019;13:336. http://dx.doi.org/10.3389/fnins.2019.00336.
[24] Csernai M, Borbély S, Kocsis K, Burka D, Fekete Z, Balogh V, et al. Dynamics of sleep oscillations is coupled to brain temperature on multiple scales. J Physiol 2019;597(15):4069–86. http://dx.doi.org/10.1113/JP277664.
[25] Kräuchi K, Cajochen C, Werth E, Wirz-Justice A. Functional link between distal vasodilation and sleep-onset latency. Am J Physiol Regul Integr Comp Physiol 2000;278(3):R741–8. http://dx.doi.org/10.1152/ajpregu.2000.278.3.R741.
[26] Dvir H, Kantelhardt JW, Zinkhan M, Pillmann F, Szentkiralyi A, Obst A, et al. A biased diffusion approach to sleep dynamics reveals neuronal characteristics. Biophys J 2019;117(5):987–97. http://dx.doi.org/10.1016/j.bpj.2019.07.032.
[27] Dvir H, Elbaz I, Havlin S, Appelbaum L, Ivanov PC, Bartsch RP. Neuronal noise as an origin of sleep arousals and its role in sudden infant death syndrome. Sci Adv 2018;4(4):eaar6277. http://dx.doi.org/10.1126/sciadv.aar6277.
[28] Kawamura H, Sawyer CH. Elevation in brain temperature during paradoxical sleep. Science 1965;150(3698):912–3. http://dx.doi.org/10.1126/science.150.3698.912.
[29] Deboer T, Franken P, Tobler I. Sleep and cortical temperature in the djungarian hamster under baseline conditions and after sleep deprivation. J Comp Physiol A 1994;174(2):145–55. http://dx.doi.org/10.1007/BF00193782.
[30] Szymusiak R. Body temperature and sleep. Handb Clin Neurol 2018;156:341–51. http://dx.doi.org/10.1016/B978-0-444-63912-7.00020-5.
[31] Gao BO, Franken P, Tobler I, Borbély AA. Effect of elevated ambient temperature on sleep, EEG spectra, and brain temperature in the rat. Am J Physiol 1995;268(6 Pt 2):R1365–73. http://dx.doi.org/10.1152/ajpregu.1995.268.6.R1365.
[32] Franken P, Tobler I, Borbély AA. Cortical temperature and EEG slow-wave activity in the rat: analysis of vigilance state related changes. Pflugers Arch 1992;420(5–6):500–7. http://dx.doi.org/10.1007/BF00374625.
[33] Sela Y, Hoekstra MM, Franken P. Sub-minute prediction of brain temperature based on sleep-wake state in the mouse. eLife 2021;10:e62073. http://dx.doi.org/10.7554/eLife.62073.
[34] Landolt HP, Moser S, Wieser HG, Borbély AA, Dijk DJ. Intracranial temperature across 24-hour sleep-wake cycles in humans. Neuroreport 1995;6(6):913–7. http://dx.doi.org/10.1097/00001756-199504190-00022.
[35] Raymann RJ, Swaab DF, Van Someren EJ. Skin deep: enhanced sleep depth by cutaneous temperature manipulation. Brain 2008;131(Pt 2):500–13. http://dx.doi.org/10.1093/brain/awm315.
[36] Whitten TA, Martz LJ, Guico A, Gervais N, Dickson CT. Heat synch: Inter- and independence of body-temperature fluctuations and brain-state alternations in urethane-anesthetized rats. J Neurophysiol 2009;102(3):1647–56. http://dx.doi.org/10.1152/jn.00374.2009.
[37] Obál FJ, Rubicsek G, Alföldi P, Sáry G. Changes in the brain and core temperatures in relation to the various arousal states in rats in the light and dark periods of the day. Pflugers Arch 1985;404(1):73–9.
[38] Alföldi P, Rubicsek G, Cserni G, Obál FJ. Brain and core temperatures and peripheral vasomotion during sleep and wakefulness at various ambient temperatures in the rat. Pflugers Arch 1990;417(3):336–41. http://dx.doi.org/10.1007/BF00371001.
[39] Campbell I. Body temperature and its regulation. Anaesth Intensive Care Med 2011;12(6):240–4. http://dx.doi.org/10.1016/j.mpaic.2008.04.009.
[40] Hanak V, Somers VK. Cardiovascular and cerebrovascular physiology in sleep. In: Handbook of clinical neurology. first ed.. vol. 98, 2011, p. 315–25. http://dx.doi.org/10.1016/B978-0-444-52006-7.00019-8.
[41] Bojarskaite L, Vallet A, Bjørnstad DM, Gullestad Binder KM, Cunen C, Heuser K, et al. Sleep cycle-dependent vascular dynamics in male mice and the predicted effects on perivascular cerebrospinal fluid flow and solute transport. Nature Commun 2023;14(1):953. http://dx.doi.org/10.1038/s41467-023-36643-5.
[42] Volgushev M, Vidyasagar TR, Chistiakova M, Yousef T, Eysel UT. Membrane properties and spike generation in rat visual cortical cells during reversible cooling. J Physiol 2000;522(Pt 1):59–76. http://dx.doi.org/10.1111/j.1469-7793.2000.0059~m.x.

[43] Jacobson GA, Diba K, Yaron-Jakoubovitch A, Oz Y, Koch C, Segev I, et al. Subthreshold voltage noise of rat neocortical pyramidal neurones. J Physiol 2005;564(Pt 1):145–60. http://dx.doi.org/10.1113/jphysiol.2004.080903.

[44] Steinmetz PN, Manwani A, Koch C, London M, Segev I. Subthreshold voltage noise due to channel fluctuations in active neuronal membranes. J Comput Neurosci 2000;9(2):133–48. http://dx.doi.org/10.1023/a:1008967807741.

[45] McGinty D, Szymusiak R. Keeping cool: a hypothesis about the mechanisms and functions of slow-wave sleep. Trends Neurosci 1990;13(12):480–7. http://dx.doi.org/10.1016/0166-2236(90)90081-k.

[46] Hayward JN, Baker MA. A comparative study of the role of the cerebral arterial blood in the regulation of brain temperature in five mammals. Brain Res 1969;16(2):417–40. http://dx.doi.org/10.1016/0006-8993(69)90236-4.

[47] Mcilvoy L. Comparison of brain temperature to core temperature: a review of the literature. J Neurosci Nurs 2004;36(1):23–31. http://dx.doi.org/10.1097/01376517-200402000-00004.

[48] Wehr TA. A brain-warming function for REM sleep. Neurosci Biobehav Rev 1992;16(3):379–97. http://dx.doi.org/10.1016/s0149-7634(05)80208-8.

[49] Pace-Schott E, Hobson J. The neurobiology of sleep: Genetics, cellular physiology and subcortical networks. Nat Rev Neurosci 2002;3(8):591–605. http://dx.doi.org/10.1038/nrn895.

[50] McCarley RW, Hobson JA. Neuronal excitability modulation over the sleep cycle: a structural and mathematical model. Science 1975;189(4196):58–60. http://dx.doi.org/10.1126/science.1135627.

[51] Steyn-Ross DA, Steyn-Ross ML, Sleigh JW, Wilson MT, Gillies IP, Wright JJ. The sleep cycle modelled as a cortical phase transition. J Biol Phys 2005;31(3–4):547–69. http://dx.doi.org/10.1007/s10867-005-1285-2.

[52] Skok K, Duh M, Stožer A, Markota A, Gosak M. Thermoregulation: A journey from physiology to computational models and the intensive care unit. Wiley Interdiscip Rev Syst Biol Med 2020;e1513. http://dx.doi.org/10.1002/wsbm.1513.

[53] Duh M, Skok K, Perc M, Markota A, Gosak M. Computational modeling of targeted temperature management in post-cardiac arrest patients. Biomech Model Mechanobiol 2022;21(5):1407–24. http://dx.doi.org/10.1007/s10237-022-01598-x.

[54] Gosak M, Milojević M, Duh M, Skok K, Perc M. Networks behind the morphology and structural design of living systems. Phys Life Rev 2022;41:1–21. http://dx.doi.org/10.1016/j.plrev.2022.03.001.

[55] Amzica F, Steriade M. Disconnection of intracortical synaptic linkages disrupts synchronization of a slow oscillation. J Neurosci 1995;15(6):4658–77. http://dx.doi.org/10.1523/JNEUROSCI.15-06-04658.1995.

[56] Zhu M, Ackerman JJ, Yablonskiy DA. Body and brain temperature coupling: the critical role of cerebral blood flow. J Comp Physiol B 2009;179(6):701–10. http://dx.doi.org/10.1007/s00360-009-0352-6.

[57] Korbo L, Pakkenberg B, Ladefoged O, Gundersen HJ, Arlien-Søborg P, Pakkenberg H. An efficient method for estimating the total number of neurons in rat brain cortex. J Neurosci Methods 1990;31(2):93–100. http://dx.doi.org/10.1016/0165-0270(90)90153-7.

[58] McIntosh R, Anderson V. A comprehensive tissue properties database provided for the thermal assessment of a human at rest. Biophys Rev Lett 2010;5(3):129–51. http://dx.doi.org/10.1142/S1793048010001184.

[59] Krilowicz BL, Edgar DM, Heller HC. Action potential duration increases as body temperature decreases during hibernation. Brain Res 1989;498(1):73–80. http://dx.doi.org/10.1016/0006-8993(89)90400-9.

[60] Attwell D, Laughlin SB. An energy budget for signaling in the grey matter of the brain. J Cereb Blood Flow Metab 2001;21(10):1133–45. http://dx.doi.org/10.1097/00004647-200110000-00001.

[61] Wang Y, Wang R, Xu X. Neural energy supply-consumption properties based on hodgkin–huxley model. Neural Plast 2017;2017:6207141. http://dx.doi.org/10.1155/2017/6207141.

[62] Tasaki I, Kusano K, Byrne PM. Rapid mechanical and thermal changes in the garfish olfactory nerve associated with a propagated impulse. Biophys J 1989;55:1033–44. http://dx.doi.org/10.1016/S0006-3495(89)82902-9.

[63] de Meis L, Bianconi ML, Suzano VA. Control of energy fluxes by the sarcoplasmic reticulum Ca2+-ATPase: ATP hydrolysis, ATP synthesis and heat production. FEBS Lett 1997;406(1–2):201–4. http://dx.doi.org/10.1016/s0014-5793(97)00244-5.

[64] Petersen PC, Vöröslakos M, Buzsáki G. Brain temperature affects quantitative features of hippocampal sharp wave ripples. J Neurophysiol 2022;127(5):1417–25. http://dx.doi.org/10.1152/jn.00047.2022.

[65] Petersen PC, Hernandez M, György B. Brain temperature affects quantitative features of hippocampal sharp wave ripples [dataset]. In: The buzsaki lab databank-public electrophysiological datasets from awake animals zenodo. 2020, http://dx.doi.org/10.5281/zenodo.4307883.

[66] Watson BO, Levenstein D, Greene JP, Gelinas JN, Buzsáki G. Network homeostasis and state dynamics of neocortical sleep. Neuron 2016;90(4):839–52. http://dx.doi.org/10.1016/j.neuron.2016.03.036.

[67] Lombardi F, Gómez-Extremera M, Bernaola-Galván P, Vetrivelan R, Saper CB, Scammell TE, et al. Critical dynamics and coupling in bursts of cortical rhythms indicate non-homeostatic mechanism for sleep-stage transitions and dual role of VLPO neurons in both sleep and wake. J Neurosci 2020;40(1):171–90. http://dx.doi.org/10.1523/JNEUROSCI.1278-19.2019.

[68] McGill R, Tukey JW, Larsen WA. Variations of box plots. Am Stat 1978;32:12–6. http://dx.doi.org/10.2307/2683468.

[69] Rayan A, Agarwal A, Samanta A, Severijnen E, van der Meij J, Genzel L. Sleep scoring in rodents: Criteria, automatic approaches and outstanding issues. Eur J Neurosci 2022;56(4):5505–22. http://dx.doi.org/10.1111/ejn.15884.

[70] Rosenthal MS, Vogel GW. The effect of a 3-day increase of ambient temperature toward the thermoneutral zone on rapid eye movement sleep in the rat. Sleep 1993;16(8):702–5. http://dx.doi.org/10.1093/sleep/16.8.702.

[71] Mrdalj J, Mattson ÅL, Murison R, Jellestad FK, Milde AM, Pallesen S, et al. Hypothermia after chronic mild stress exposure in rats with a history of postnatal maternal separation. Chronobiol Int 2013;31(2):252–64. http://dx.doi.org/10.3109/07420528.2013.846351.

[72] Nelson A, Faraguna U, Zoltan J, Tononi G, Cirelli C. Sleep patterns and homeostatic mechanisms in adolescent mice. Brain Sci 2013;3(4):318–43. http://dx.doi.org/10.3390/brainsci3010318.

[73] Boulant JA. Role of the preoptic-anterior hypothalamus in thermoregulation and fever. Clin Infect Dis 2000;31(Suppl 5):S157–61. http://dx.doi.org/10.1086/317521.

[74] Ramsay DS, Woods SC. Clarifying the roles of homeostasis and allostasis in physiological regulation. Psychol Rev 2014;121(2):225–47. http://dx.doi.org/10.1037/a0035942.

[75] Halász P, Terzano M, Parrino L, Bódisz R. The nature of arousal in sleep. J Sleep Res 2004;13:1–22. http://dx.doi.org/10.1111/j.1365-2869.2004.00388.x.

[76] Lõhmus M. Possible biological mechanisms linking mental health and heat: A contemplative review. Int J Environ Res Public Health 2018;15(7):1515. http://dx.doi.org/10.3390/ijerph15071515.

[77] Li J, Vitiello MV, Gooneratne NS. Sleep in normal aging. Sleep Med Clin 2018;13(1):1–11. http://dx.doi.org/10.1016/j.jsmc.2017.09.001.